Dynamical heterogeneity in lattice glass models

Richard K. Darst,[1] David R. Reichman,[1,a)] and Giulio Biroli[2]

[1]*Department of Chemistry, Columbia University, 3000 Broadway, New York, New York 10027, USA*
[2]*Institut de Physique Théorique, CEA, IPhT, F-91191 Gif-sur-Yvette, France
and CNRS, URA 2306, F-91191 Gif-sur-Yvette, France*

In this paper, we consider in detail the properties of dynamical heterogeneity in lattice glass models (LGMs). LGMs are lattice models whose dynamical rules are based on thermodynamic, as opposed to purely kinetic, considerations. We devise a LGM that is not prone to crystallization and displays properties of a fragile glass-forming liquid. Particle motion in this model tends to be locally anisotropic on intermediate time scales even though the rules governing the model are isotropic. The model demonstrates violations of the Stokes–Einstein relation and the growth of various length scales associated with dynamical heterogeneity. We discuss future avenues of research comparing the predictions of LGMs and kinetically constrained models to atomistic systems. © *2010 American Institute of Physics*. [doi:10.1063/1.3298877]

I. INTRODUCTION

The cause of the dramatic slowing of dynamics close to the empirically defined glass transition is a subject of great continued interest and debate.[1,2] Different theoretical proposals have been put forward aimed at describing some or all of the phenomena commonly observed in experiments and computer simulations.[3–13] While these proposals are often based on completely divergent viewpoints, many of them are able to rationalize the same observed behaviors. This fact stems from the somewhat limited amount of information available from experiments and simulations. Since the growth of relaxation times in glassy systems is precipitous, it is very difficult, and in some cases impossible, to distinguish models solely on the basis of different predictions of gross temperature dependent relaxation behavior. In addition, computer simulations, which are often more detailed than experiments, are limited by the range of times scales and sizes of systems that can be studied. These difficulties have hindered the search for a consensus on the microscopic underpinnings of vitrification.

Despite the continued debate that revolves around the theoretical description of supercooled liquids and glasses, little argument exists regarding the importance of dynamical heterogeneity as a key feature of glassy behavior.[14–19] Dynamical heterogeneity refers to the fact that as a liquid is supercooled, dynamics become starkly spatially heterogeneous, requiring the cooperative motion of groups of particles for relaxation to occur. Dynamical heterogeneous motion manifests in several ways, and leads to violations of the Stokes–Einstein relation,[20–24] cooperative hopping motion reflected in nearly exponential tails in particle displacement functions,[3,25–28] and growing length scales such as those associated with the recovery of Fickian diffusion,[29–32] growing multipoint correlation functions.[7,33–41] Indeed, the relatively recent explication of the phenomena of dynamical

heterogeneity has dramatically shifted the focus of the field and has placed new constraints on the necessary ingredients for a successful theory of glass formation.

Given the similarity of some aspects of dynamical heterogeneity to critical fluctuations in standard critical phenomena, it is natural to investigate two and three dimensional simplified coarse-grained models that encode the crucial features of this heterogeneity. Currently, the most investigated class of coarse-grained models are the "kinetically constrained models" (KCMs).[3,4,42–44] KCMs are spin or lattice models that generate slow, glassy relaxation via constraints on the dynamical moves that are allowed. The slowing down of the dynamics is caused by rarefactions of facilitating regions, also called defects. Importantly, although the dynamics is complex, the thermodynamics is trivial since the dynamical rules are such that all configurations are equally likely. The philosophy of this viewpoint is that thermodynamic quantities, such as the configurational entropy, are not the fundamental underlying cause of the growing time scales in supercooled liquids. It has been argued that the quantitative disagreement[45] between thermodynamic features of KCMs and real experiments is of little dynamical consequence.[46] In support of this perspective is the fact that KCMs have been remarkably successful in generating features of dynamical heterogeneity such as Stokes–Einstein decoupling, growing dynamical length scales, and excess tails in the real-space particle displacement function.[22,31,47,48]

On the other hand, one may wonder if a deeper viewpoint would allow for an understanding of the kinetic rules that govern particle motion in the supercooled liquids. It is natural to speculate that such aspects might have roots in the thermodynamics of configurations. Indeed, simple local Monte Carlo "dynamics" can reproduce all features of dynamical heterogeneity seen in Newtonian molecular dynamics simulations, and are based simply on making local moves that are *configurationally* allowed.[49] Lattice models based on this concept are called "lattice glass models" (LGMs), and were first considered by Biroli and Mézard.[50] The rules for

---

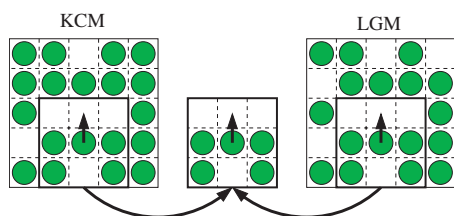a)Electronic mail: reichman@chem.columbia.edu.

FIG. 1. Comparison and distinction of a caricature of a KCM with a LGM. In the KCM, any configuration is allowed, but move may only be made if a particle has at least one missing neighbor before and after the move. In the LGM, the global configuration is defined such that all particles must have at least one missing neighbor, and all dynamical moves must respect this rule. Note that the local environment around the moving particle is identical in this example, while the global configurations are distinct. Periodic boundary conditions are assumed for both panels.

such models seem at first sight like that of KCMs. For example, in the simplest versions of such models, a particle may move if it is surrounded by no more than a fixed number of nearest neighbors before and after the move.[51–54] Locally, this is identical to the type of dynamical constraint that appears in the KCMs introduced by Kob and Andersen (KA).[43] However, this constraint must be met globally: *all* particles must have no more than a fixed number of nearest neighbors. As the density of the system increases, fewer and fewer configurations exist for which these constraints may be satisfied. It is thus the entropy of configurations that governs the slowing of dynamics, intimately connecting the nontrivial thermodynamic weight of states accessible to the local dynamics. Indeed, LGMs can be solved exactly within the Bethe approximation, or on Bethe lattices,[50,53] and have been shown to have a glass transition due to the vanishing of the configurational entropy. The distinction between the KCM and LGM viewpoint is illustrated in Fig. 1.

LGMs have been studied by a number of groups, but the focus has not generally been on real-space aspects of dynamical heterogeneity. For example, Coniglio and co-workers have developed a simple LGM that avoids crystallization and displays many features of typical glass-forming materials, including a growing multipoint susceptibility $[\chi_4(t)]$.[53,54] On the other hand, this system appears to behave as a strong glass-former, with a stretching parameter close to one, and exhibits essentially no Stokes–Einstein violation. Our goal in this work is to survey, in detail, the dynamical behavior of a new LGM which bears similarity to the original Biroli–Mézard model but is not prone to crystallization. The main conclusion that we draw is that LGMs are at least as realistic as KCMs in their description of all commonly studied features of dynamical heterogeneity. In this regard, simple coarse-grained lattice models based on the thermodynamic weight of states are no less viable as fundamental caricatures of glassy liquids than are KCMs based on weights of trajectories. We conclude our work by highlighting several key ways that LGMs and KCMs may be distinguished. We reserve the investigation of these comparisons for a future study. Our paper is organized as follows. Section II outlines the model. Section III discusses both simple averaged dynamics as well as aspects of dynamical heterogeneity. In Sec. IV, we conclude with a discussion of the meaning of our findings and the future directions to be pursued.

II. MODEL

Here, we define the LGM that forms the basis of our simulations. The original model of Biroli–Mézard is quite prone to crystallization.[50] This fact makes its use problematic for the study of glassy behavior since crystallization always intervenes before supercooling becomes significant. The crystallization problem persists on a square lattice for all binary mixtures we have studied. However, we have found that certain generalizations of the Biroli–Mézard model with three species of particles are stable against crystallization for the densities that are sufficiently high that glassy dynamics may be clearly observed.

Our model follows the original rules of the Biroli–Mézard model. Particles exist on a cubic periodic lattice of side $L=15$ and each lattice site can contain only zero or one particle. All particles, at all times, must satisfy the condition *a particle of type "m" must have m or fewer neighbors of any type*. A neighbor is considered any particle in one of the $2d$ (d=dimensionality) closest lattice sites along the cubic coordinate axes.[55]

The particular three species model we employ is defined by 10% type 1 particles, 50% type 2 particles, and 40% type 3 particles. We denote this model the "t154" model to indicate its basis in thermodynamics and to specify the types and percentages of each particle. The composition of t154 model was determined via trial and error by picking particle types with clashing crystallization motifs thereby frustrating crystallization. Crystallization was monitored by inspection of the angle resolved static structure factor, direct inspection of configurations, and by monitoring bulk thermodynamic quantities.

As discussed in the introduction, there appear to be strong similarities between the rules that govern KCMs such as the KA model and the t154 model.[43] For example, both models employ constraints with a maximum number of neighbors, but in the KA model this restriction only applies to the *mobile* particles, while in the t154 model applies to *all* particles. Our model does not require any special dynamics methods. We employ local canonical Monte Carlo "dynamics" via primitive translational moves.[49] Note that for the t154 model the energy can only be zero (no packing violations) or infinite (packing violation or overlap), thus the acceptance criteria reduce to rejection if there is a packing violation and acceptance otherwise. This allows us to implement an event-driven algorithm which accelerates the simulation of lattice dynamics.[56]

For thermodynamic studies, we employ grand-canonical Monte Carlo with both translational moves as well as particle insertion/deletion. Figure 2 contains a plot of the density of the system as a function of the chemical potential of type 1 particles. Models which crystallize (such as original binary model of Biroli–Mézard) have a sharp jump in this curve at the crystallization point. Clearly, this feature is absent in the t154 model. For comparison, both curves are displayed.[57]
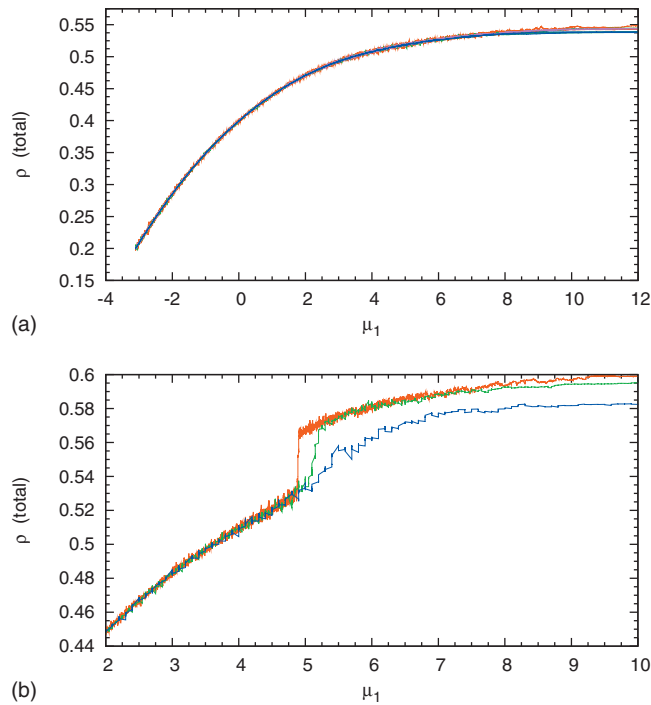
FIG. 2. Crystallization thermodynamics in LGM. Top: The t154 model. μ_1 refers to the chemical potential of the type 1 particles. The maximum density observed for the 15^3 lattice is 0.5479 (exactly 1849 out of 3375 lattice sites occupied). The three plotted quenching rates vary between a 0.01 and 0.05 increase of μ_1 per 10000 cycles. Bottom: A close up of the equivalent plot for the BM model. Note the clear discontinuity upon crystallization. Slower μ-increase rates produce a sharper discontinuity.

FIG. 3. Decay of the self-intermediate scattering function $F_s(k,t)$ for $k'=5$ $[k=(2\pi/L)k']$. Densities are 0.3, 0.4, 0.45, 0.48, 0.50, 0.51, 0.52, 0.53, 0.535, 0.5375, 0.5400, 0.5425 from fastest relaxation to slowest relaxation. These densities are used in all plots in this paper unless otherwise indicated. Top: Plotted on a linear-log scale. Bottom: Same data as upper panel plotted on a log$\{-\log_{10}[F_s(k,t)]\}$ vs log(t) scale. Lowest density curves are at the top left.

III. DYNAMICAL BEHAVIOR

A. Simple bulk dynamics

In this subsection, we describe the behavior of a simple 2-point observable, namely the self-intermediate scattering function,[58] defined as

$$F_s(k,t) = \left\langle \frac{1}{N}\sum_i e^{i\mathbf{k}\cdot[\mathbf{r}_i(t)-\mathbf{r}_i(0)]} \right\rangle. \tag{1}$$

We measure $F_s(k,t)$ only for the type 2 particles which are present in the greatest fraction for the three distinct species. Throughout this paper, we report k-vectors using k', where $k=(2\pi/L)k'$. We have checked that $F_s(k,t)$ is qualitatively similar for the other species of particles. The relaxation of $F_s(k,t)$ of the system at the wavevector $k'=5$ ($k=2\pi/3$) for various densities is shown in Fig. 3. The bulk of the decay may be fit to a stretched exponential function, $F_s(k,t)=\exp\{-[t/\tau_\alpha(k)]^{\beta(k)}\}$. As is customary, the alpha-relaxation time is found by the value $F_s(\tau_\alpha)=1/e$ and the $\beta(k)$ exponent is determined by a direct fit to the terminal decay. We find that for densities below approximately $\rho=0.48$ the value of β saturates at the expected value $\beta=1$ characteristic of simple nonglassy dynamics, while for the highest density simulated, $\beta=0.7$. This behavior, over a similar range of supercooling, is reminiscent of the behavior found in atomistic models of glass-forming liquids.[59,60] In order to better reveal the relaxat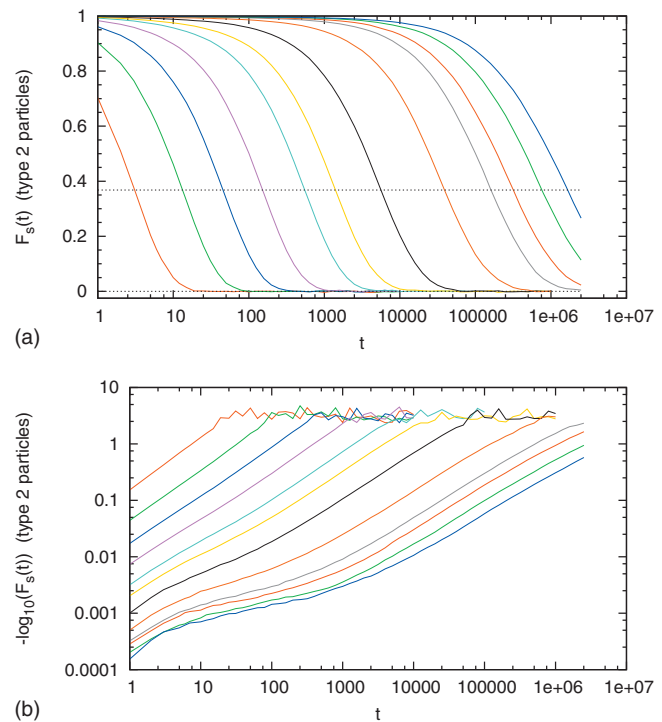ion behavior, $F_s(t)$ is also displayed on a log-log versus log-time scale. In this plot, the slope of the long time growth is related to the exponent β. We have found that the values of β extracted from the slopes of the long time portion of the log-log versus log plot indeed coincide with that found by a direct fit to a stretched exponential form. At the highest densities, a shoulder appears in the short time relaxation. This feature is indicative of a secondary relaxation feature perhaps akin to beta relaxation in realistic glass-forming liquids. It should be noted, however, that the amplitude of this feature is very close to unity. This is quantitatively distinct from the plateau values expected in atomistic off-lattice models[59,60] and even LGMs with more complicated lattice degrees of freedom,[53,54] but is similar to that encountered in simple spin models such as variants of the random orthogonal model.[61]

As is typical of fragile glass-forming systems, the t154 model exhibits relaxation times that do not follow the (generalized) Arrhenius form.[62] This behavior is illustrated in Fig. 4. At low densities, plots of log(τ) versus ρ indeed follow a straight line, however, in the vicinity of $\rho \sim 0.5$, the plot of τ versus ρ deviates from this straight line and the functional density dependence of the relaxation time becomes much more precipitous. While we have not attempted to quantitatively characterize this density dependence, it should be noted that the onset of increased sensitivity to changes in density occurs is the same narrow window that marks the noticeable decrease in the values of the stretching exponent β.
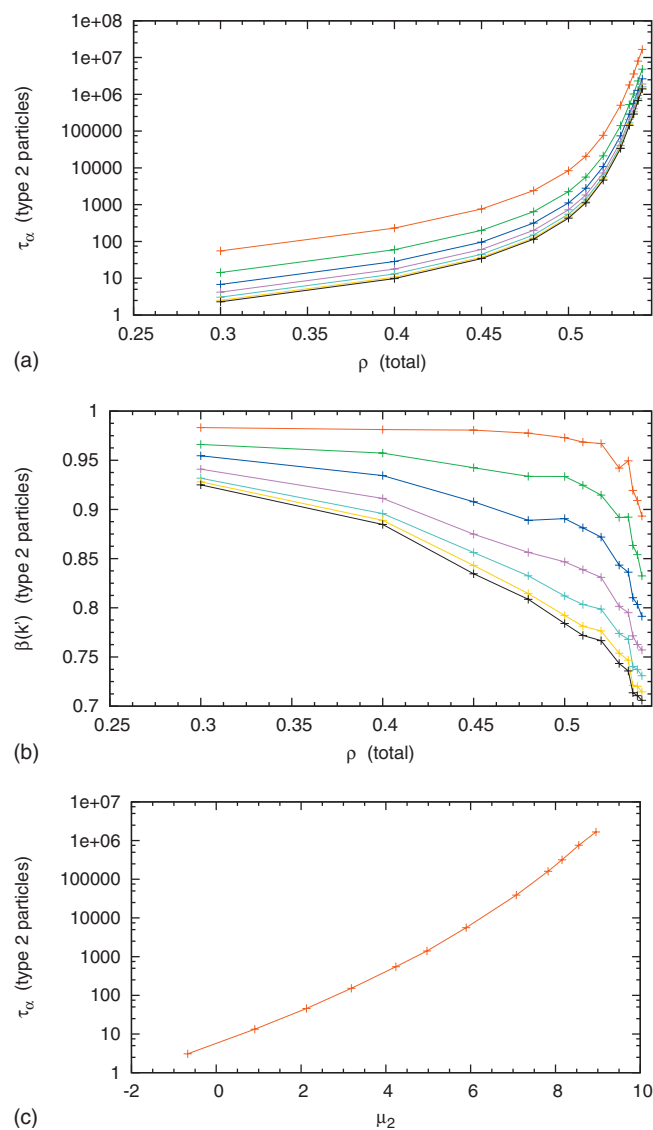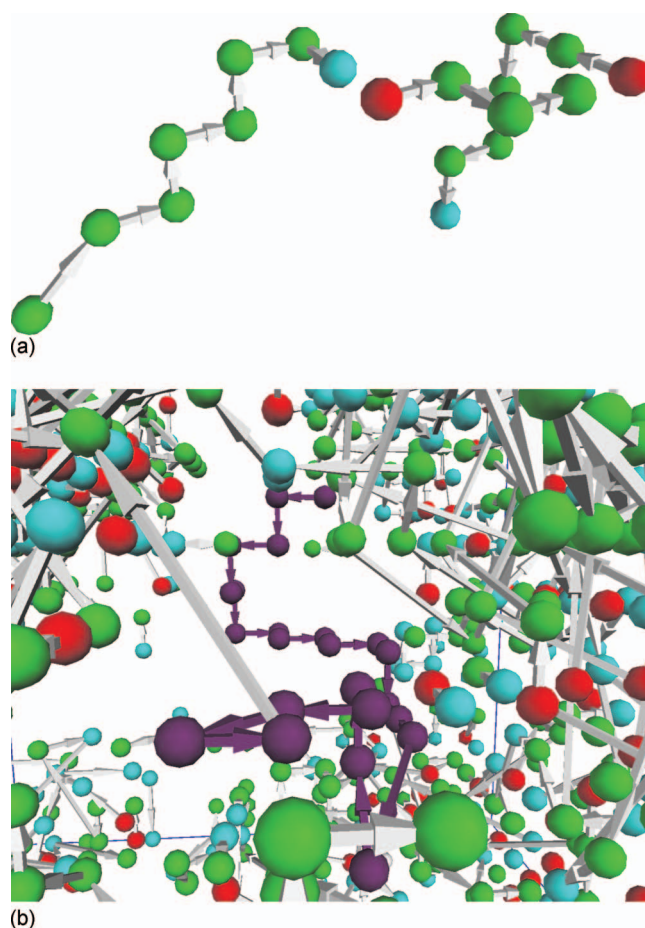
FIG. 5. Examples of stringlike motion apparent in the t154 model. (a) An example of a string with all neighboring particles removed. (b) A similar string in the context of other particles. Note that the string here is truly isolated in space, away from other mobile particles. In these figures, type 1 particles are white, type 2 particles are blue, and type 3 are green. Sites occupied at the initial time but vacated at the final time are shown in red. These pictures show only the differences in position of particles between the origin of time and the final time, not the path the particles took to achieve that displacement. All figures are at a density of 0.5400, with Δt times in (a) 251, (b) 199 526. The α-relaxation time for $k'=5$ at this density is about 7.8×10^6.

FIG. 4. Top: τ_α (time at which $F_s(k,t)=1/e$) as a function of density, ρ. Plotted for $k'=1,2,3,4,5,6,7$, with lowest k at the top. Center: Beta stretching exponent of $F_s(k,t)$ [from terminal fits $F_s(k,t) \sim \exp(-(t/\tau_\alpha)^\beta)$]. Lowest k curve is at the top of the plot. Bottom: Plot of log scale τ_α against chemical potential μ of type 2 particles. The behavior is consistent with $\tau_\alpha=5.7 \exp[-21\mu_2/(\mu_2-24)]$.

B. Motion on the atomic scale

We begin our discussion of the nature of heterogeneous dynamical behavior in the t154 LGM by observing the qualitative details of particle motion under supercooled conditions. This will set the stage for analysis of quantitative measures of dynamical heterogeneity in the model. For the sake of comparison, we also investigate the analogous behavior in the KA model. This comparison is useful because it suggests how models with similar local rules but different global rules (rooted in either the purely kinetic or thermodynamic basis of the particular model) may give rise to distinct dynamics at the particle scale.

We start by simply observing the patterns of mobility in real space starting from a set initial condition of the t154 model found at a given density after equilibration. A similar analysis has been performed recently by Chaudhuri et al. for the KA model, where no equilibration is required since all

initial configurations with a set density of defects are allowed.[63] For a theoretical description of the dynamics of the KA model, see Ref. [64]. We note that, as expected, the t154 model exhibits regions of spatially localized particle activity against a backdrop of transiently immobilized particles. A rather remarkable feature of the patterns of mobility in this model is that we find evidence of stringlike motion, where a group of particles moves over a short distance, each taking the place of the previous particle in the string.[65,66] This motif can be seen mostly on timescales less than the α-relaxation time, but occasionally stringlike motion may be seen to persist on longer timescales. This behavior is demonstrated in Fig. 5.

The behavior of particle motion observed in the KA model is somewhat different than that seen in the t154 model as described above. As in the t154 model, and as observed by Chaudhuri et al., motion in the KA model shows similar activity regions in the vicinity of defect sites giving rise to heterogeneous motion (Fig. 6). However, the boundaries be-
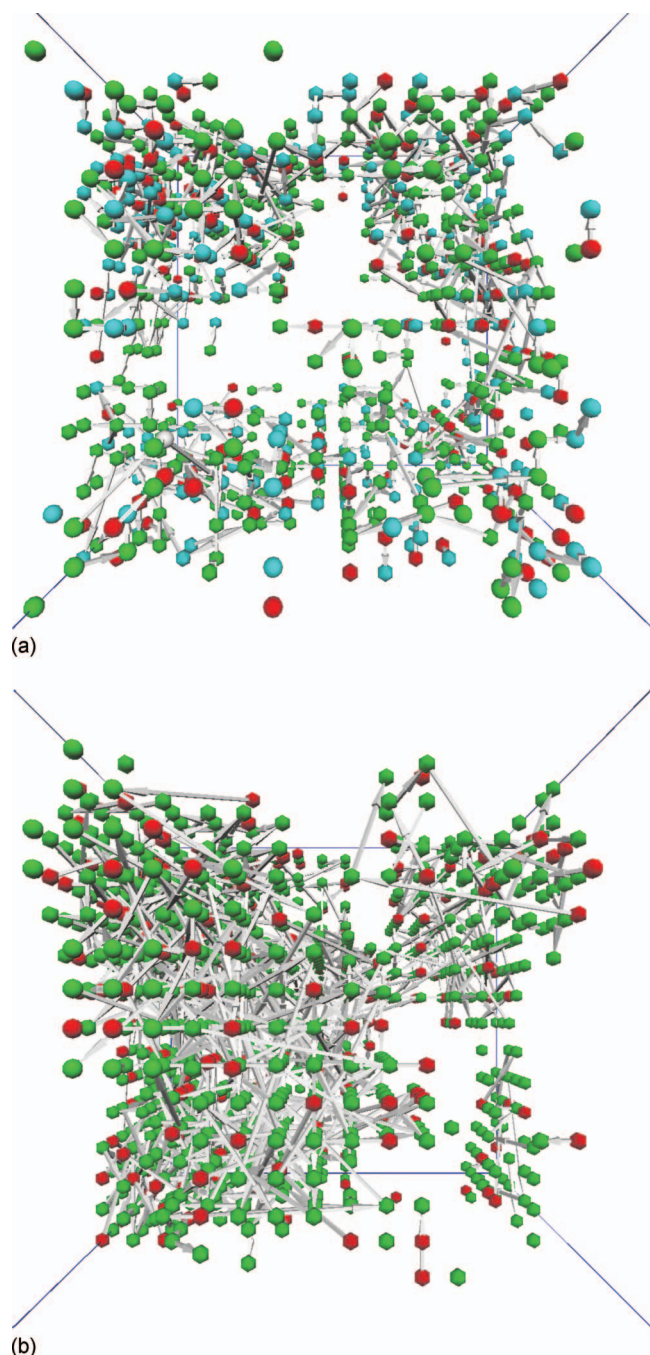
FIG. 6. Examples cluster shapes in the (a) the t154, model, density $\rho=.5400$ and (b) the KA model, density $\rho=.8500$. Arrows indicate motion between initial and final times. Time separation is 1/10th of the α-relaxation time. In the t154 model, we see more fractal and disconnected clusters, while in the KA model, mobile domains tend to be smoother clusters.

tween active and inactive regions at comparable timescales appear to be more distinct in the KA model. Furthermore, the particle scale motion in the KA is much more isotropic, exhibiting much fewer cases of directional mobility compared with the t154 model. It would be interesting to compare the two models by quantifying this difference via the type of directional multipoint correlators devised by Doliwa and Heuer.[67] It is not clear if the difference between the models is related to the fundamental distinction between LGMs and KCMs or just the specifics of the particular models considered. In particular, the t154 is a multicomponent model, un-

like the KA model. The stringlike motion on short time scales seems to occur predominantly on the rather rough boundaries of slow clusters.[68] This behavior, reminiscent of the picture of dynamic heterogeneity that put forward by Stillinger,[69] might be strongly influenced by compositional heterogeneity. A useful way to address general issues related to how the initial configuration constrains subsequent dynamics would be a systematic isoconfigurational ensemble analysis comparing LGMs and KCMs.[70] This will be the topic of a future publication.[71]

In the next few sections, we discuss how some of the most important indicators of dynamical heterogeneity in supercooled liquids manifest in the t154 model. The quantities that we discuss are the magnitude of violations of the Stokes–Einstein relation, exponential tails (indicative of hopping transport) in the van Hove function, the existence of a Fickian length scale and the development of a dynamical length scale quantified by the multipoint function $S_4(q,t)$. Unless otherwise stated, specific correlation functions and transport coefficients are calculated with respect to type 2 particles.

C. Stokes–Einstein violation

In typical fluids, a mean-field linear-response relationship asserts that the product of the tracer particle diffusion constant and the fluid viscosity divided by the temperature is a constant.[58] This connection between diffusion and dissipation is known as the Stokes–Einstein relationship, and empirically is known to hold even at the atomic scale in liquids over a wide range of densities and temperatures. In supercooled liquids, the Stokes–Einstein relation generally does not hold.[20–25,72,73] In fact, the product of the diffusion constant and the viscosity of a liquid may exceed that expected from the Stokes–Einstein relation by several orders of magnitude close to the glass transition. There are many theoretical explanations for Stokes–Einstein violations in supercooled liquids, which essentially all invoke dynamical heterogeneity as the fundamental factor leading to the breakdown of the simple relationship between diffusion and viscosity. It should be noted that similar relationships hold between the diffusion constant and the self and collective time constants associated with the decay of density fluctuations. In this work, we focus on the relaxation time of the self-intermediate scattering function defined above as our proxy for the fluid viscosity.

It is well known that the product $D\tau_\alpha$, where τ_α is the α-relaxation time of the self-intermediate scattering function, shows a strong temperature/density dependence in both realistic atomic simulations as well as in the class of KCMs that describe fragile glass-forming liquids. No direct studies of this quantity have been made in LGMs. The LGM of Coniglio and co-workers would appear to show essentially no Stokes–Einstein violations because the diffusion constant and the relaxation time may both be fit to power laws with exponents that have, within numerical accuracy, the same magnitude.[53,54] This, however, is not surprising since many of the features of the model resemble those of a strong glass-forming system, where violations of the Stokes–Einstein re-
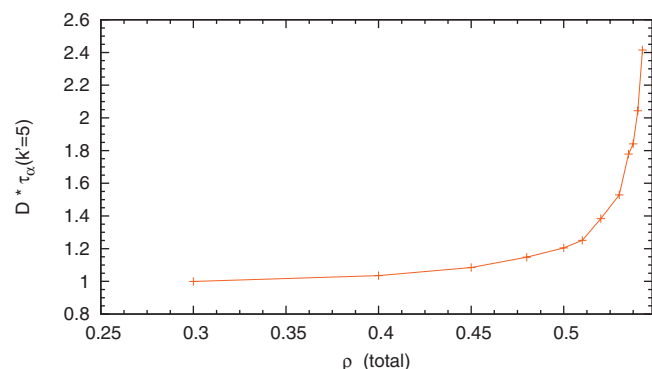
FIG. 7. Violation of the Stokes–Einstein relation, $D\tau_\alpha \sim$ constant, using τ_α at $k'=5$. Data has been normalized to $D\tau_\alpha=1$ at the lowest density.

FIG. 8. van Hove function for $\rho=.5375$ and various times. Distances are measured independently along each coordinate axis. The times plotted, from left to right, are 10^5, 316227 (approximately the α-relaxation time), and 10^6. An exponential fit to the tail of the $t=316227$ case is shown by a dotted line.

lation are, at most, weak. The features of the t154 model with regard to nonexponential relaxation and the density dependence of the relaxation time τ_α indicate that this model behaves more like a fragile glass-former. Thus, we expect clear violations of the Stokes–Einstein relation. Indeed, as shown in Fig. 7, $D\tau_\alpha$ increases markedly as density is increased. Over the range densities that we can access, the magnitude of the violation is very similar to that seen in the canonical KA Lennard-Jones (KALJ) mixture over a comparable range of changes in relaxation time.[27] Interestingly, violations begin to become pronounced at densities similar to where the relaxation times and stretching exponents become strongly sensitive to increased density. Thus, a consistent onset density is observed as in more realistic atomistic systems.

D. van Hove function

It is now rather well established that an additional "quasiuniversal" feature of dynamical heterogeneity near the glass transition is contained in the shape of the real-space van Hove function.[26–29] In particular, it has been argued that the tails of the self van Hove function should be approximately exponential in form. These "fat tails" imply that the rare particles that do undergo large displacements exist in populations in excess of what would be expected in a purely Gaussian displacement distribution. While non-Gaussian tails should be expected of any distribution for the wings that fall outside of limits of bounds set by the central limit theorem, the palpable exponential tails in supercooled liquids imply large non-Gaussian effects indicative of transport that is strongly affected by heterogeneous hopping motion.

Here, we demonstrate that such effects occur in the t154 model in a manner similar to that seen both in experiments in colloidal and granular systems as well as in computer simulations of atomic systems. Figure 8 shows the self part of the real-space van Hove function,

$$G_s(x,t) = \langle \delta\{x - |\hat{\mathbf{x}} \cdot [\mathbf{r}_i(t) - \mathbf{r}_i(0)]|\} \rangle, \qquad (2)$$

for the type two particles in the t154 model. Because we are on a lattice, we restrict our distances along the three coordinate axes $\hat{\mathbf{x}}$ individually in our calculation. We see that for times of the order of the α-relaxation time, these tails are clearly visible. For very long or short time scales, the shape of the tail deviates somewhat from the more exponential
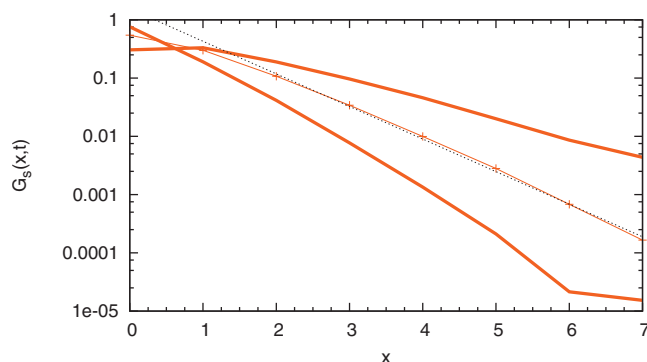
form exhibited at intermediate times. This behavior is quite similar to that seen in simulations of atomistic systems,[27,28] and is fully consistent with the behavior found in KCMs.[25]

E. Fickian length

Related to the existence of excess tails in the van Hove function is the existence of a length scale that characterizes the anomalous transport. More specifically, the exponential tails in the van Hove function are distinguished from the Gaussian form of the displacement distribution obtained at relatively short distances for fixed times. The crossover from Fickian to non-Fickian behavior should be characterized by time scales as well as *length scales* over which this crossover occurs. A non-Fickian length scale may be defined by examining the k-dependent diffusion constant $D(k)=1/(\tau_\alpha k^2)$.[30–32] The wavevector that characterizes the crossover from the expected diffusive behavior to an anomalous regime is inversely related to such a length scale. In Fig. 9, we plot $D(k')$. Clearly, as the density is increased, the length scale separating the Fickian and non-Fickian regimes increases. This behavior is consistent with that found in KCMs and simulations of atomistic glass-forming liquids. It should be noted that Stokes–Einstein violations, the development of exponential tails in the self van Hove function, and a well-developed Fickian length scale are all manifestations of related aspects of dynamically heterogeneous motion in supercooled liquids.[27]
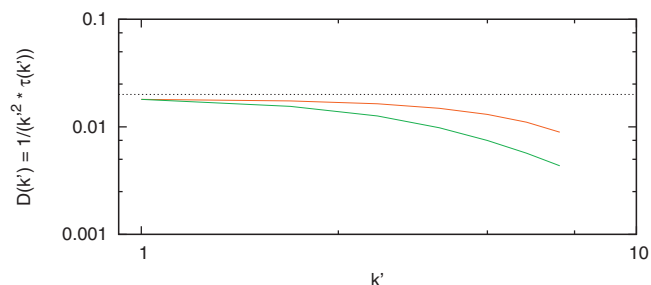

FIG. 9. k-dependent diffusion constant$=1/[k'^2\tau_\alpha(k)]$. Densities of 0.3000 (upper) and 0.5425 (lower). The higher density curve is multiplied by a scale factor of 2.992×10^5 for ease of comparison. A dotted flat line is included for reference of behavior expected in the purely Fickian case.

F. χ_4 and S_4 fluctuation measures

The Fickian length scale is merely one length scale that arises naturally in systems where dynamics become increasingly heterogeneous. Perhaps more fundamental is the growth of dynamical length scales associated with multipoint correlations of the dynamics. Supercooled liquids do not show simple static correlations that would indicate a growing correlation length. It should be noted that this does not exclude growing static correlations of a more complex kind, for example point-to-set correlations.[7,38,74] Regardless, cooperativity in dynamics may be measured via first defining a local overlap function[3,17,33,35,36]

$$\delta f_k(q,t) = \frac{1}{N}\sum_i e^{i\mathbf{q}\cdot\mathbf{r}_i(0)}(\cos\{\mathbf{k}\cdot[\Delta\mathbf{r}_i(t)]\} - F_s(k,t)), \quad (3)$$

where $\Delta\mathbf{r}_i(t) = \mathbf{r}_i(0) - \mathbf{r}_i(t)$. $f_k(q,t)$ is defined for one configuration, and the average is over all $\mathbf{k}$ and $\mathbf{q}$ with the magnitudes k and q. Then, $S_4(q)$ is defined as

$$S_4(q) = N\langle|\delta f_k(q,t)|^2\rangle \quad (4)$$

where this average is over the most general ensemble of configurations.[36] The χ_4 value is defined as the limit $S_4(q\to0)$. $\chi_4(t)$ may be calculated strictly at $q=0$ from

$$\chi_4(t) = N\langle|\delta f_k(q=0,t)|^2\rangle, \quad (5)$$

where the average is over the entire ensemble and all $\mathbf{k}$ consistent with the magnitude of k. Note that, as discussed in Ref. 36, the value of $\chi_4(t)$ computed in this manner is a lower bound for the extrapolation of $S_4(q\to0,t)$.

The quantity $S_4(q,t)$ is a multipoint dynamical analog of $S(q)$. Just as the low q behavior of $S(q)$ indicates a growing (static) length scale in systems approaching a second order phase transition, scattering from dynamically heterogeneous regions undergoing cooperative motion will manifest growth in the amplitude of the low q region of $S_4^{ol}(q,t)$, indicative of the size scale of the dynamical correlations for systems approaching the glass transition.

The behavior of the quantity $S_4^{ol}(q,t)$ is shown in Fig. 10. Only type 2 particles have been used in the calculation. As can clearly be seen, for densities above $\rho \sim 0.5$ which constitutes the onset density of this system, the low q behavior shows a marked upturn as $q\to0$. The growth of $S_4^{ol}(q,t)$ as $q\to0$, as density is increased, suggests a growing length scale as supercooling progresses. This nontrivial behavior is what is found in atomistic simulated systems. Future work will be devoted to a precise characterization of the length scale that may be extracted from $S_4^{ol}(q,t)$ in the t154 model so that a comparison may be made with recent work detailing the behavior of this length in realistic off-lattice systems.[41,75]

IV. CONCLUSION

In this paper, we have presented a new LGM based on the original Biroli–Mézard model.[50] Via the introduction of an additional species of particle, we have demonstrated that our model is stable against crystallization. This fact allows us to study sufficiently high density configurations that manifest
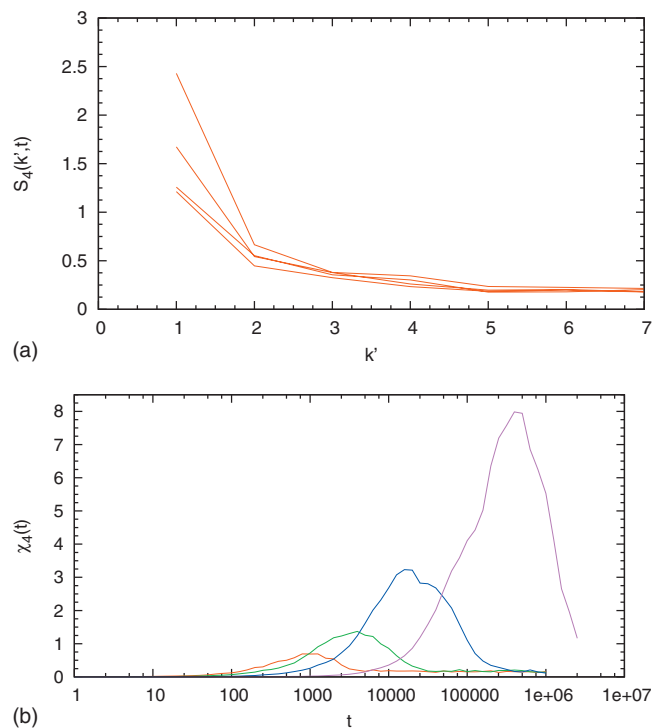

FIG. 10. Top: Plot of $S_4(q,t)$ at τ_α for densities 0.51, 0.52, 0.53, and 0.54. Bottom: Plot of $\chi_4(t)$ for the same densities. Peak values correspond to lower bounds for of the value of $S_4(q,t)$ in the upper panel at $q=0$.

features of dynamical heterogeneity. Unlike some previous LGMs, our model exhibits the canonical features of a fragile glass-former. In terms of the gross features of relaxation behavior, our LGM shows behavior similar to the standard KALJ mixture. In particular, we find that the degree of violation of the Stokes–Einstein relation and the magnitude of stretching in the decay of the self-intermediate scattering function track the relaxation times at densities above the onset of supercooling in a manner consistent with that seen in the KALJ system. Features of dynamical heterogeneity such as exponential tails in the van Hove function, the growth of a dynamical length scale as quantified by the function $S_4(q,t)$, Stokes–Einstein violations, and the emergence of a Fickian length scale all occur in a manner expected from experiments and simulations of fragile glass-forming liquids.

The similarity between the description of dynamic heterogeneity found in KCMs and LGMs stands in stark contrast to the underlying foundations of the models themselves. As emphasized in the introduction, KCMs are based on a constrained dynamics for which the number of available dynamical paths leading to relaxation becomes increasingly rare as the density increases and the number of defects decrease. In KCMs, all real-space configurations at a fixed number of defects (excluding rare blocked configurations) are equally likely. On the other hand, LGMs are based on transitions between real-space configurations that become increasingly scarce as the density is increased. This is not to say that there is not a facilitated-like dynamics in LGMs. On the contrary, as we have demonstrated in Sec. III, local and sometimes anisotropic dynamics may be generated naturally in LGMs without the explicit introduction of facilitating defects. An important message that emerges from this study is

that *the phenomenology of dynamic heterogeneity is not sufficient to distinguish pictures or validate models based on transitions between sets of states in configuration space from those based on sets of paths in space time.*

How then might these pictures be differentiated? While contrasting competing models that generate seemingly similar dynamical behavior is a difficult endeavor, several possible studies might be useful for this task. Here, we outline four avenues that could provide key information that distinguish the purely dynamical picture from one based on transitions thermodynamic states.

(a) *The mosaic length scale:* The random first order theory of Wolynes and co-workers posits the existence of a static length scale which is defined by the region over which particles are pinned by the surrounding self-generated amorphous configuration.[6,7,38] This length scale also exists in KCMs, but it is decoupled from the relaxation dynamics of the system.[76] Recent atomistic computer simulations have successfully located the mosaic length scale.[38] It would be quite useful to perform an analysis similar to that devised by Jack and Garrahan for LGMs.[76] Since LGMs are based on the entropy of real-space configurations, it is expected that, here, the mosaic length does couple to the glassy dynamics. Since LGMs are much simpler than atomistic off-lattice models, the direct study of the mosaic length (and point-to-set correlations in general) in LGMs might provide key avenues for the testing of the putative coupling between relaxation and such length scales in simulated atomistic systems.

(b) *Correlations between configurational entropy and dynamics:* Empirical correlations between the configurational entropy and the α-relaxation time have been noted for many years, and this correlation lies at the heart of several prominent theories. Such correlations are still widely debated, but seem to hold at least crudely in many glass-forming systems.[77,78] LGMs should be expected to exhibit such correlations, while it is known that KCMs do not exhibit such correlations. Recently, Karmakar *et al.*[41] purported to show that finite-size effects of the α relaxation time follow precisely the Adam–Gibbs relation between the configurational entropy and the α-relaxation time in the KALJ system. If true, such correlations would be a challenge to KCMs, since it is difficult to envision how the configurational entropy would track the α-relaxation time for different system sizes if it were not a crucial component of relaxation phenomena. Such correlations, however, are subtle to measure since the Adam–Gibbs relationship is an exponential one and the apparent correlation could depend on the somewhat indirect computational method used in Ref. 41 to define the configurational entropy. It would be most useful to investigate such effects in the simpler LGMs, which might provide a cleaner means of isolating the configurational entropy. It should be noted that finite size effects do appear to follow an approximate Adam–Gibbs relationship in at least one other lattice model.[79] Such

studies might spur more detailed investigations in simulated atomistic systems thus allowing for a clear comparison between LGMs, KCMs and more realistic systems.

(c) *Single-particle and collective predictability ratios:* In an important piece of work, Jack and Berthier devised metrics that access the degree to which single particle and collective dynamics are deterministically predicted by a set initial configuration over a given time scale.[80] KCMs and LGMs differ in how allowed configurations are constructed. KCMs have explicit defects, while configurations in LGMs are determined by global constraints, and thus do not contain explicit defects. Since the very composition of initial conditions differ markedly in these models, one expects that the metrics defined by Jack and Berthier would behave differently in KCMs and LGMs. Thus, it would be very profitable to examine the density and temperature dependence of the single particle and collective predictability ratios in KCMs and LGMs as a possible means of distinguishing between state-based and dynamical constraint-based pictures.[71]

(d) *Evolution of the facilitation mechanism approaching the glass transition:* Although in both KCM and LGM pictures facilitation plays an important role in the relaxation of the system, a peculiar and different temperature and density evolution is expected. In particular, in the KCM picture, facilitation is due to the motion of mobility regions or defects. Dynamics slows down, and concomitantly dynamic heterogeneity increases, because these regions become rarer approaching the glass transition. A crucial assumption is that these defects are conserved or at least that nonconservation is a rare event that becomes rarer at lower temperature/high density. These assumptions impose important constraints on the evolution of the facilitation mechanism. Thus, it would be very interesting to examine this issue for example using the cluster analysis developed in Ref. 81 to study the relaxation dynamics of granular systems.

Investigation of these and other studies aimed at distinguishing the underlying pictures that LGMs and KCMs are based on will be the subject of future work.

ACKNOWLEDGMENTS

[1] P. Debenedetti and F. Stillinger, Nature (London) **410**, 259 (2001).
[2] M. Ediger, C. Angell, and S. Nagel, J. Phys. Chem. **100**, 13200 (1996).
[3] J. Garrahan and D. Chandler, Phys. Rev. Lett. **89**, 035704 (2002).
[4] J. Garrahan and D. Chandler, Proc. Natl. Acad. Sci. U.S.A. **100**, 9710 (2003).

[5] L. Hedges, R. Jack, J. Garrahan, and D. Chandler, Science **323**, 1309 (2009).

[6] V. Lubchenko and P. G. Wolynes, Annu. Rev. Phys. Chem. **58**, 235 (2007).

[7] J. Bouchaud and G. Biroli, J. Chem. Phys. **121**, 7347 (2004).

[8] D. Kivelson, S. A. Kivelson, X. Zhao, Z. Nussinov, and G. Tarjus, Physica A **219**, 27 (1995).

[9] W. Gotze and L. Sjogren, Rep. Prog. Phys. **55**, 241 (1992).

[10] K. Schweizer and E. Saltzman, J. Chem. Phys. **119**, 1181 (2003).

[11] J. Dyre, Rev. Mod. Phys. **78**, 953 (2006).

[12] J. Langer, Phys. Rev. Lett. **97**, 115704 (2006).

[13] A. Heuer, J. Phys. Condens. Matter **20**, 373101 (2008).

[14] S. Butler and P. Harrowell, J. Chem. Phys. **95**, 4454 (1991).

[15] M. Hurley and P. Harrowell, Phys. Rev. E **52**, 1694 (1995).

[16] W. Kob, C. Donati, S. Plimpton, P. Poole, and S. Glotzer, Phys. Rev. Lett. **79**, 2827 (1997).

[17] R. Yamamoto and A. Onuki, Phys. Rev. E **58**, 3515 (1998).

[18] K. Schmidt-Rohr and H. Spiess, Phys. Rev. Lett. **66**, 3020 (1991).

[19] M. Ediger, Annu. Rev. Phys. Chem. **51**, 99 (2000).

[20] I. Chang and H. Sillescu, J. Phys. Chem. B **101**, 8794 (1997).

[21] M. Cicerone and M. Ediger, J. Chem. Phys. **104**, 7210 (1996).

[22] Y. Jung, J. Garrahan, and D. Chandler, Phys. Rev. E **69**, 061205 (2004).

[23] X. Xia and P. Wolynes, J. Phys. Chem. B **105**, 6570 (2001).

[24] G. Tarjus and D. Kivelson, J. Chem. Phys. **103**, 3071 (1995).

[25] L. Berthier, D. Chandler, and J. Garrahan, Europhys. Lett. **69**, 320 (2005).

[26] D. Stariolo and G. Fabricius, J. Chem. Phys. **125**, 064505 (2006).

[27] P. Chaudhuri, L. Berthier, and W. Kob, Phys. Rev. Lett. **99**, 060604 (2007).

[28] E. Saltzman and K. Schweizer, Phys. Rev. E **77**, 051504 (2008).

[29] S. F. Swallen, K. Traynor, R. J. McMahon, M. D. Ediger, and T. E. Mates, J. Phys. Chem. B **113**, 4600 (2009).

[30] L. Berthier, Phys. Rev. E **69**, 020201 (2004).

[31] A. Pan, J. Garrahan, and D. Chandler, Phys. Rev. E **72**, 041106 (2005).

[32] G. Szamel and E. Flenner, Phys. Rev. E **73**, 011504 (2006).

[33] N. Lačević, F. Starr, T. Schrøder, and S. Glotzer, J. Chem. Phys. **119**, 7372 (2003).

[34] C. Dasgupta, A. Indrani, S. Ramaswamy, and M. Phani, Europhys. Lett. **15**, 307 (1991).

[35] S. Franz and G. Parisi, J. Phys.: Condens. Matter **12**, 6335 (2000).

[36] L. Berthier, G. Biroli, J. Bouchaud, W. Kob, K. Miyazaki, and D. Reichman, J. Chem. Phys. **126**, 184503 (2007).

[37] S. Franz and A. Montanari, J. Phys. A **40**, F251 (2007).

[38] G. Biroli, J. Bouchaud, A. Cavagna, T. Grigera, and P. Verrocchio, Nat. Phys. **4**, 771 (2008).

[39] L. Berthier, G. Biroli, J. Bouchaud, L. Cipelletti, D. Masri, D. L'Hote, F. Ladieu, and M. Pierno, Science **310**, 1797 (2005).

[40] G. Biroli, J. Bouchaud, K. Miyazaki, and D. Reichman, Phys. Rev. Lett. **97**, 195701 (2006).

[41] S. Karmakar, C. Dasgupta, and S. Sastry, Proc. Natl. Acad. Sci. U.S.A. **106**, 3675 (2009).

[42] G. Fredrickson and H. Andersen, Phys. Rev. Lett. **53**, 1244 (1984).

[43] W. Kob and H. Andersen, Phys. Rev. E **48**, 4364 (1993).

[44] F. Ritort and P. Sollich, Adv. Phys. **52**, 219 (2003).

[45] G. Biroli, J. Bouchaud, and G. Tarjus, J. Chem. Phys. **123**, 044510 (2005).

[46] D. Chandler and J. Garrahan, J. Chem. Phys. **123**, 044511 (2005).

[47] L. Hedges and J. Garrahan, J. Phys. A: Math. Theor. **41**, 324006 (2008).

[48] L. Hedges and J. Garrahan, J. Phys. Condens. Matter **19**, 205124 (2007).

[49] L. Berthier, Phys. Rev. E **76**, 011507 (2007).

[50] G. Biroli and M. Mézard, Phys. Rev. Lett. **88**, 025501 (2001).

[51] G. McCullagh, D. Cellai, A. Lawlor, and K. Dawson, Phys. Rev. E **71**, 030102 (2005).

[52] K. Dawson, S. Franz, and M. Sellitto, Europhys. Lett. **64**, 302 (2003).

[53] M. Pica Ciamarra, M. Tarzia, A. de Candia, and A. Coniglio, Phys. Rev. E **67**, 057105 (2003).

[54] M. Pica Ciamarra, M. Tarzia, A. de Candia, and A. Coniglio, Phys. Rev. E **68**, 066111 (2003).

[55] It should be noted that LGMs of the type described here involve extreme constraints that must be globally satisfied and are thus not realistic translations of off-lattice particle-based models. Such constraints might indeed induce artificial behavior, especially at higher densities. It would be most interesting to investigate "soft" versions of such models where constraints may be locally violated at the cost of an energy penalty. In this regard, such models would be the configurational analog of KCMs where dynamical constraints may be broken at the cost of an energy penalty. D. Chandler and J. P. Garrahan, "Dynamics on the Way to Forming Glass: Bubbles in Space-Time," Annu. Rev. Phys. Chem. (in press).

[56] A. Bortz, M. Kalos, and J. Lebowitz, J. Comput. Phys. **17**, 10 (1975).

[57] A subtle issue arises in the nature of glassy behavior observed in the t154 model outlined in this work. LGMs could have a dynamical percolation-like transition, as in the spiral model.[82] This has been indeed found in some LGMs on the Bethe lattice[83] and would slow down the dynamics for reasons completely different from the diminishing of the configurational entropy. If there is a low-lying crystal phase then one can show that this dynamical percolation-like transition cannot take place in finite dimension. Although we have not found a crystal phase for the model, the existence of such a transition seems unlikely and irrelevant for our present work. First, it can be shown that blocked structures, if they exist, have to verify much more constraints than in the spiral model.[82] Second, we have found that the relaxation time growth of the persistence functions with increasing density in local canonical Monte Carlo simulations are similar to those under grand-canonical dynamics, which cannot contain any blocked structure. The union of these two facts render the dynamical blocking scenario highly unlikely.

[58] U. Balucani and M. Zoppi, *Dynamics of the Liquid State* (Oxford University Press, New York, 1994).

[59] W. Kob and H. Andersen, Phys. Rev. E **51**, 4626 (1995).

[60] G. Wahnström, Phys. Rev. A **44**, 3752 (1991).

[61] T. Sarlat, A. Billoire, G. Biroli, and J. Bouchaud, J. Stat. Mech.: Theory Exp. **2009**, P08014).

[62] L. Berthier and T. A. Witten, Europhys. Lett. **86**, 10001 (2009).

[63] P. Chaudhuri, S. Sastry, and W. Kob, Phys. Rev. Lett. **101**, 190601 (2008).

[64] C. Toninelli, G. Biroli, and D. Fisher, Phys. Rev. Lett. **92**, 185504 (2004).

[65] C. Donati, J. Douglas, W. Kob, S. Plimpton, P. Poole, and S. Glotzer, Phys. Rev. Lett. **80**, 2338 (1998).

[66] C. Donati, S. Glotzer, P. Poole, W. Kob, and S. Plimpton, Phys. Rev. E **60**, 3107 (1999).

[67] B. Doliwa and A. Heuer, J. Phys. Condens. Matter **11**, 025 (1999).

[68] G. Appignanesi, J. Rodríguez Fris, R. Montani, and W. Kob, Phys. Rev. Lett. **96**, 057801 (2006).

[69] F. Stillinger, J. Chem. Phys. **89**, 6461 (1988).

[70] A. Widmer-Cooper, P. Harrowell, and H. Fynewever, Phys. Rev. Lett. **93**, 135701 (2004).

[71] R. K. Darst, D. R. Reichman, and G. Biroli (unpublished).

[72] F. Stillinger and J. Hodgdon, Phys. Rev. E **50**, 2064 (1994).

[73] C. Liu and I. Oppenheim, Phys. Rev. E **53**, 799 (1996).

[74] M. Mézard and A. Montanari, J. Stat. Phys. **124**, 1317 (2006).

[75] R. Stein and H. Andersen, Phys. Rev. Lett. **101**, 267802 (2008).

[76] R. Jack and J. Garrahan, J. Chem. Phys. **123**, 164508 (2005).

[77] R. Richert and C. Angell, J. Chem. Phys. **108**, 9016 (1998).

[78] L. Martinez and C. Angell, Nature (London) **410**, 663 (2001).

[79] A. Crisanti and F. Ritort, Europhys. Lett. **51**, 147 (2000).

[80] L. Berthier and R. Jack, Phys. Rev. E **76**, 041509 (2007).

[81] R. Candelier, O. Dauchot, and G. Biroli, Phys. Rev. Lett. **102**, 088001 (2009).

[82] G. Biroli and C. Toninelli, Eur. Phys. J. B **64**, 567 (2008).

[83] O. Rivoire, G. Biroli, O. Martin, and M. Mezard, Eur. Phys. J. B **37**, 55 (2003).